Comparative assessment of safety indicators for vehicle trajectories on highways

Mullakkal-Babu, Freddy Antony; Wang, Meng; Farah, Haneen; van Arem, Bart; Happee, Riender

DOI
10.3141/2659-14

Publication date
2017

Document Version
Final published version

Published in
Transportation Research Record

Comparative Assessment of Safety Indicators for Vehicle Trajectories on Highways

Freddy Antony Mullakkal-Babu, Meng Wang, Haneen Farah, Bart van Arem, and Riender Happee

Safety measurement and its analysis have been challenging and well-researched topics in transportation. Conventionally, surrogate safety measures have been used as safety indicators in simulation models for safety assessment, in control formulations for driver assistance systems, and in data analysis of naturalistic driving studies. However, surrogate indicators give partial insights on traffic safety; that is, these indicators only indicate a predetermined set of possible precrash situations for an interacting vehicle pair. Recently, a safety indicator called the "driving safety field," based on field theory, was proposed for two-dimensional vehicle interactions. However, the objectivity of its functional form and its validity have yet to be tested. A qualitative and quantitative comparison of different safety indicators was provided as a risk measure to demarcate their mathematical properties and evaluate their usefulness in quantifying trajectory risk. Five relevant safety indicators were compared: inverse time to collision, postencroachment time, potential indicator of collision with urgent decceleration, warning index, and safety field force. Their formulations were mathematically analyzed to yield qualitative insights and their values over simulated vehicle trajectories were evaluated to yield quantitative insights. The results acknowledge the limitations and demarcate the functional utilities of the selected safety indicators.

Safety is a key performance indicator of any transportation system. Road safety research has received considerable attention because of the enormous societal losses incurred in road accidents worldwide, with about 1.25 million fatalities and between 20 million and 50 million nonfatal injuries (*1*). Recent efforts in safety research are primarily focusing on the use of surrogate safety measures (SSMs) as a proactive and cost-efficient method to evaluate safety; the limitations are acknowledged of using crash records (*2*) such as road safety assessment (*3, 4*), ex ante safety evaluation in driver assistance and automation systems (*5, 6*), and behavior modeling of human drivers in safety-critical scenarios (*7*). The advent of intelligent vehicles has brought uncertainties, especially with regard to vehicle interactions. The uncertainties stem from the fact that an intelligent vehicle possesses enhanced communication and control capabilities compared with a regular vehicle but lacks the spatial and temporal anticipative capabilities. Achieving agreement on a set of objective safety indicators that are applicable in mixed traffic is a methodological challenge. Hence, the selection of a safety indicator has profound implications for the quality and agreement of safety research findings.

Essentially, a safety indicator is a measure of risk associated with vehicle interaction. SSMs are the most common risk indicators used in safety studies. The risk delineated by an SSM could vary depending on the formulation and parameter consideration. More important, SSMs are often discontinuous because their validity is limited to a prescribed set of interacting vehicle configurations. For example, time to collision is not defined in a car-following situation with a faster leader. Recently, a safety model was proposed that is capable of describing risk continuously over the vehicle path. This safety model is based on field theory and defines driving risk as a spatial field (*8*). However, the objectivity of its functional form and its validity are yet to be tested. Therefore, despite the wide range of safety indicators, selection of an appropriate indicator warranting validity and agreeable results is intricate.

Safety indicators are usually selected on the basis of their study scope and methodological suitability; this restriction makes it difficult to generalize the findings. Even though safety indicators have been extensively reviewed and empirically validated in the past, limited literature exists on the demarcation of their mathematical properties, representation of risk causal factors in their formulation, and evaluation of their usefulness in quantifying trajectory risk. To that end, this study compares relevant safety indicators with regard to their qualitative and quantitative aspects. Their formulations are mathematically analyzed to yield qualitative insights and their values over simulated vehicle trajectories are evaluated to yield quantitative insights. The results acknowledge the limitations and demarcate the functional utilities of SSMs.

LITERATURE REVIEW

Crash statistics have been traditionally used for road safety evaluation. Even though relevant, they have drawbacks such as the unavailability of sufficient crash data to derive statistically significant conclusions and the inability of their use for ex ante evaluation. These drawbacks made researchers turn toward a complementary approach that uses SSMs. The characteristics of SSMs are that they are more frequent

F. A. Mullakkal-Babu, M. Wang, H. Farah, and B. van Arem, Department of Transport and Planning, Faculty of Civil Engineering and Geosciences, Delft University of Technology, Stevinweg 1, 2628 CN Delft, Netherlands. R. Happee, Department of Biomechanical Engineering, Faculty of Mechanical, Maritime, and Materials Engineering, Delft University of Technology, Mekelweg 2, 2628 CD Delft, Netherlands. Corresponding author: F. A. Mullakkal-Babu, F.A.Mullakkalbabu@tudelft.nl.

Transportation Research Record: Journal of the Transportation Research Board, No. 2659, 2017, pp. 127–136.
http://dx.doi.org/10.3141/2659-14

than crashes, they are observable in traffic, and they represent crash causality and crash mechanisms (*9*).

SSMs have been critically and extensively reviewed over time (*6, 10–13*). Generally, these measures define the collision risk of an interacting vehicle pair as a function of their instantaneous kinematic states (acceleration, velocity, and position) and they depend on the spatial configuration. Hence, these indicators can be categorized into longitudinal and lateral indicators on the basis of the location of the interacting vehicles. Longitudinal indicators have been widely used in forward collision warning systems, safety assessment of highways, and human behavioral modeling in rear-end crash scenarios. Common longitudinal SSMs are time to collision (TTC), inverse time to collision (iTTC), time exposed time to collision, time integrated time to collision (*14*), deceleration required to avoid collision, and potential indicator of collision with urgent deceleration (PICUD) (*12*). Lateral SSMs like postencroachment time (PET) have been used as a risk measure in lane change controllers, safety assessment of intersections, and lateral vehicle maneuvers.

SSMs that are not intrinsically bounded to lateral or longitudinal interactions can be found in the literature. For instance, the crash potential index and the aggregated crash index are based on a predetermined set of probable evasive maneuvers (*6, 15*). The functionality of these probabilistic indicators is restricted to certain driving regimes because of the difficulty of exhaustively listing all possible maneuvers. In addition, predictive risk maps have been proposed to estimate the future risk based on the predicted trajectories of interacting vehicles (*16*). Even though this approach is efficient for ex ante safety evaluation in controllers, its performance inherently depends on the prediction modules and does not fall within the scope of the current work. Recently, Wang et al. proposed an alternative risk assessment methodology for two-dimensional vehicle interactions based on field theory (*8*). They model risk as a vector field and incorporate road, vehicle, and driver characteristics into a unified field formulation. In the current study, the focus is on five safety indicators: iTTC, PICUD, a warning index (relevant longitudinal indicators with different parameter considerations), PET (relevant lateral indicator), and safety field force (two-dimensional safety indicator).

QUALITATIVE ANALYSIS

Qualitative analysis of the selected indicators was performed with the following objectives: to evaluate the mathematical properties of their functional form in a multivehicle scenario and to benchmark their formulation with expected causal tendencies of major risk-contributing variables.

Desirable Mathematical Properties for Risk Measure in Multivehicle Scenario

In this section the desirable mathematical properties of safety indicators are presented to verify the applicability of selected safety indicators in multivehicle scenarios. Mathematical measure theory has prescribed criteria for a function to be termed as a measure (*17*). As risk measures of vehicle interaction, it is desirable for safety indicators to adhere to these criteria.

Let X be the set of all interacting vehicles V under consideration, and Σ be the collection of possible subsets of X. A risk measure $\mu: \Sigma \rightarrow R$ from Σ to the real number line R is a mathematical risk measure if the following conditions are satisfied:

- Nonnegativity. The risk measure μ of any vehicle V with index k in Σ is a nonnegative value:

$$\mu(V_k) \geq 0 \tag{1}$$

This property is desirable considering that a negative risk value is nonintuitive and its use is ambiguous in multivehicle scenarios (i.e., it could cancel a positive risk value).

- Countable additivity. The risk measure μ should indicate the union of risk values due to the interacting vehicles M in a multivehicle scenario in which the risk measure of a countable disjoint collection of vehicle units $\{V_i\}_{i=1}^{M}$ is the same as the sum of all risk measures of each vehicle unit as follows:

$$\mu\left(\bigcup_{k=1}^{M} V_k\right) = \sum_{k=1}^{M} \mu(V_k) \tag{2}$$

This property simplifies the individual risk calculations for complex multivehicle interactions, and it allows the addition of individual risk measures to estimate the total societal and collective risk. However, countable additivity is not an essential property to indicate the risk associated with the interaction of a vehicle pair like car following.

Risk Factors and Expected Causal Tendencies

As to the major contributing factors of risk and their expected causal tendencies, the expectation is based on reasoning and relationships that have been reported in previous empirical and physics-based crash studies. Dynamics and causality of a crash are directly and indirectly influenced by various factors, and it would be farfetched to list them exhaustively. However, few of these factors have been reported to have a causal relationship with vehicle collisions. First, the probability of a collision between two road users is expected to increase with their approaching speed rate and to decrease with the intervehicle spacing (a shorter time for the driver to react and less possibility of risk mitigation or an evasive maneuver). Second, the collision impact is expected to increase with an increase in velocity (*18*) and mass (*19*) of the conflicting vehicles (with higher vehicular velocity, the driver should react more rapidly to avoid a collision; higher vehicular mass results in higher kinetic energy transferred and higher collision severity). Third, the collision impact is reported to increase with delta-V, or the change in vehicle velocity as the result of an impact (*20*). Finally, roadway characteristics like surface friction (*21*) and driver characteristics like reaction time (*22*) are expected to influence the collision risk.

Benchmarking Safety Indicators with Expected Risk Tendencies

In this section, the expected risk tendency of a factor is compared with the risk tendency as described by the partial derivative of the indicator with respect to the factor.

TTC

"TTC" is defined as the time required for two vehicles to collide if they continue in their present velocity along the present path:

$$\text{TTC} = \frac{s_n}{\Delta v_n} \qquad v_n > v_{n-1}$$

where v_n denotes the instantaneous velocity of the vehicle n, and $\Delta v_n = v_n - v_{n-1}$ and s_n denote the relative velocity and forward spacing of vehicle n with respect to the front vehicle $n-1$. iTTC is the inverse formulation of TTC and is widely used in controllers like the adaptive cruise controller (*23*) and to assess human driver behavior (*24*). A higher value represents higher risk and the interaction risk is often captured by the minimum TTC or maximum iTTC over the interaction period. It is formulated as follows:

$$\text{iTTC} = \frac{v_n - v_{n-1}}{s_n} \qquad \text{if } v_n > v_{n-1} \tag{3}$$

The increased risk with an increase in the approach rate is

$$\frac{\partial \text{iTTC}}{\partial \Delta v} = \frac{\partial \text{iTTC}}{\partial \Delta v_n} = \frac{1}{s_n} > 0$$

The decreased risk with an increase in the spacing of the slower leader is

$$\frac{\partial \text{iTTC}}{\partial s_n} = \frac{-\Delta v}{s_n^2}$$

As shown in Table 1, both these indications are in agreement with the expected risk tendencies.

PICUD

"PICUD" is defined as the forward spacing between two vehicles if both of them brake with a maximum deceleration (*12*) as follows:

$$\text{PICUD} = s_n + \frac{v_{n-1}^2 - v_n^2}{2a_{\max}} - t_h v_n \tag{4}$$

where $a_{\max}$ denotes the maximum deceleration and t_h denotes the time delay of the human response; a smaller PICUD indicates higher risk. The risk increases with an increase in approach rate, vehicle velocity, and human reaction time:

$$\frac{\partial \text{PICUD}}{\partial \Delta v} = -\frac{v_n + v_{n-1}}{2a_{\max}} < 0$$

$$\frac{\partial \text{PICUD}}{\partial v_n} = -\left(\frac{v_n}{a_{\max}} + t_h\right) < 0$$

and

$$\frac{\partial \text{PICUD}}{\partial t_h} = -v_n < 0$$

$\partial \text{PICUD}/\partial s = 1 > 0$ indicates that the risk decreases at a constant rate with an increase in spacing. As shown in Table 1, PICUD is in agreement with the expected risk tendencies.

Warning Index

The warning index (w) is a safety indicator used in collision warning algorithms (*23*). This indicator includes factors like tire–road friction and system delay. A lower w represents higher risk and it is formulated as follows:

$$w = \frac{s_n - d_{\text{br}}}{d_w - d_{\text{br}}} \tag{5}$$

$$d_{\text{br}} = \Delta v_n t_s + f(\mu)\left(\frac{v_n^2 - v_{n-1}^2}{2a_{\max}}\right) \tag{6}$$

$$d_w = \Delta v_n t_s + f(\mu)\left(\frac{v_n^2 - v_{n-1}^2}{2a_{\max}}\right) + v_n t_h \tag{7}$$

where

d_{br} = required braking distance,
d_w = required warning distance,
$f(.)$ = friction scaling function,
μ = estimated value of tire–road friction, and
t_s = system delay.

TABLE 1 Theoretical Verification of Safety Indicators

Aspect	Factors	Expected Tendency	iTTC	PICUD	Warning Index	Safety Force
Proximity to point of collision	Relative velocity Spacing	Increase Decrease	Increase Decrease	Increase Decrease	Increase Decrease	Increase Decrease
Collision impact	Vehicle velocity Vehicle mass	Increase Increase	Increase na	Increase na	Increase subject to the condition na	Increase Increase
Roadway characteristics	Surface friction	Decrease	na	na	Decrease subject to condition	Decrease
Human factors	Reaction time	Increase	na	Increase	Increase	Increase
Range	na	na	(0, ∞)	(−∞, +∞)	(0, ∞)	(0, ∞)

NOTE: na = not applicable.

The decreasing w indicates increasing risk. The risk increases with an increase in approach rate and human reaction time, as follows:

$$\frac{\partial w}{\partial \Delta v} = -\frac{f(\mu)(v_n + v_{n-1})}{2a_{\max} v_n t_h} - \frac{t_s}{v_n t_h} < 0$$

$$\frac{\partial w}{\partial t_h} = -\frac{w}{t_h} < 0$$

The risk decreases with an increase in spacing:

$$\frac{\partial w}{\partial s} = \frac{1}{v_n t_h} > 0$$

As shown in Table 1, w is in agreement with the expected risk tendencies. However, there are some relations that contradict the expected risk tendencies:

$$\frac{\partial w}{\partial v_n} > 0$$

is subject to the following condition:

$$\frac{\Delta v_n t_s}{v_n^2 t_h} < \frac{s}{v_n^2 t_h} + \frac{f(\mu)}{2a_{\max} t_h} + \frac{f(\mu) v_{n-1}^2}{2a_{\max} t_h v_{n-1}^2}$$

$$\frac{\partial w}{\partial \mu} = \frac{v_n^2 - v_{n-1}^2}{2a_{\max} v_n t_h} > 0$$

if $f(\mu)$ is an increasing function of μ. This formula indicates that the risk increases with an increase in the road friction coefficient while approaching a faster leader.

PET

PET is used as a risk measure in scenarios involving lateral maneuvers. It denotes the time lapse between the end of the encroachment of the turning vehicle and the time when the vehicle actually arrives at the potential point of collision (*25*). The encroachment line x^e in the case of a lane-changing maneuver is defined as a virtual line perpendicular to the lane-dividing marker and crossing the intersection point of the lane-dividing marker and the lane change trajectory. To understand the variation of PET chronologically, the encroachment line and the corresponding PET are predicted at every time step using kinematic prediction with constant velocity assumption. When two vehicles pass the encroachment line one after the other, the PET definition as per the previous assumption is as follows:

$$\text{PET} = \frac{x^e - x_j}{v_j} - \frac{x^e - x_i}{v_i} \tag{8}$$

where x_j and v_j are the position and velocity of the first vehicle, respectively, and x_i and v_i are the position and velocity of the second vehicle, respectively. The longitudinal position of the encroachment line is x^e. Since this formulation does not directly involve Δv, the mathematical properties are not analyzed further.

Driving Safety Field

Field theory has been used to model traffic flow (*26*). In this theory, moving road objects such as vehicles and not-moving road objects such as lane markings are represented as component fields and their union represents the total driving risk. On the basis of field theory, Wang et al. proposed a driving safety field (*8*); the driving safety field of a road object is a physical field that denotes its influence on driving safety. This influence is determined by the driver behavior characteristics, road condition, attributes, and kinematic state of the road object. The magnitude and direction of this influence are denoted by the field strength vector. A vehicle in the aforementioned field experiences a safety field force (SF), which denotes its current driving risk. The proposed field strength and field force for two moving vehicles are given as follows:

$$\boldsymbol{E}_{cj} = kR_c M_c (1 + DR_c) e^{k_1 v_c \cos\theta} \frac{1}{|\boldsymbol{r}_{cj}|^{k_3}} \cdot \frac{\boldsymbol{r}_{cj}}{|\boldsymbol{r}_{cj}|} \tag{9}$$

$$\boldsymbol{F}_{cj} = \boldsymbol{E}_{cj} \cdot R_j M_j (1 + DR_j) e^{-k_1 v_j \cos\varnothing} \tag{10}$$

where

$\boldsymbol{E}_{cj}$, $\boldsymbol{F}_{cj}$ = safety field strength vector and safety field force vector, respectively, on vehicle j because of moving vehicle c;
$\boldsymbol{r}_{cj}$ = radial distance vector from vehicle c to vehicle j;
θ (clockwise positive) = angle between directions v_c and $\boldsymbol{r}_{cj}$;
$\varnothing$ = angle between directions v_j and $\boldsymbol{r}_{cj}$; and
k, k_1, k_3 = calibration coefficients.

DR_i: $i \in \{c, j\}$ denotes the driver risk factor and is a dimensionless value between 0 (safe driver) and 1 (risk-taking driver). M_i: $i \in \{c, j\}$ denotes the virtual mass of a moving or nonmoving object and is parameterized by its physical mass, vehicle type, and velocity. R_i : $i \in \{c, j\}$ denotes the factor that influences the road condition and is parameterized by road–tire friction coefficient, curvature, slope, and visibility. In this study, the values of the parameters as suggested by Wang et al. were used (*8*). Figure 1 demonstrates the spatial distribution of the safety field strength caused by vehicle c. A larger $\boldsymbol{F}_{cj}$ (in blue) means a higher driving risk for vehicle j.

The risk increases with an increase in approach rate:

$$\frac{\partial \boldsymbol{F}_{cj}}{\partial \Delta v} = k_1 \boldsymbol{F}_{cj} > 0$$

The risk decreases with an increase in spacing:

$$\frac{\partial \boldsymbol{F}_{cj}}{\partial \boldsymbol{r}_{cj}} = k_3 \boldsymbol{F}_{cj} |\boldsymbol{r}_{cj}|^{k_3 - 1}$$

The original work by Wang et al. provides a detailed formulation of R_i, DR_i, and M_i (*8*). If R_i is defined as an increasing function of $f(\mu)$, $\boldsymbol{F}_{cj}$ decreases with the road friction coefficient. If DR_i is defined as an increasing function of t_h, $\boldsymbol{F}_{cj}$ increases with human reaction time. If M_i is defined as an increasing function of v_n, $\boldsymbol{F}_{cj}$ increases with vehicular velocity. This status holds for vehicular

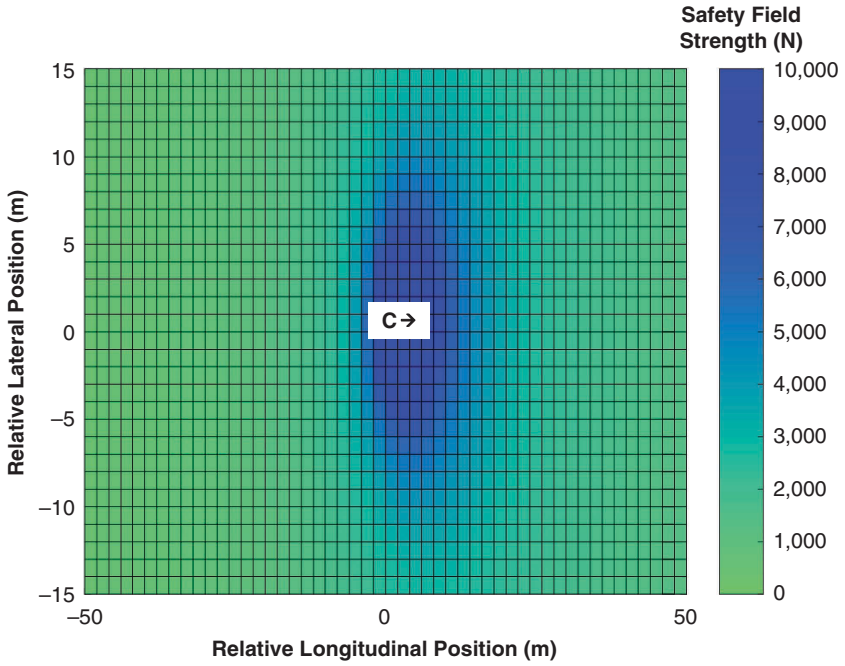

FIGURE 1 Demonstration of SF strength due to moving vehicle (blue indicates higher risk; unit of field strength is newtons).

mass as well. As shown in Table 1, the indications are in agreement with the expected tendencies.

Findings of Qualitative Analysis

The theoretical verification of the five safety indicators just described reveals the following:

- The selected indicators have limited consideration of risk factors and the SF formulation incorporates the largest number of factors;
- The selected indicator formulations represent the expected risk tendencies; however, a contradiction was found in the case of the w (Table 1); and
- The selected SSMs do not account for vehicle mass in their formulation.

Examination of the mathematical properties of the selected indicators reveals the following:

- None of the selected safety indicators can claim a countable additivity property since they are defined for vehicle pairs. Even though the SF on a vehicle is additive, in its present vector formulation, the risk due to the presence of multiple vehicles cannot be added. For example, forces acting in opposite directions tend to cancel out, but the risk measure due to two vehicles cannot cancel out.
- PICUD and PET can have a negative risk value, which is undesirable in a multivehicle scenario (Table 1).
- Quantitatively, iTTC, w, and SF may go to infinity at limiting conditions (Table 1). Even though this property is theoretically plausible, it violates the principle of countable additivity and necessitates an upper-bound definition. For instance, a risk measure tending to infinity is computationally undesirable for adaptive cruise control systems (*23*).

Figure 2 plots the forward spacing versus relative velocity representing the vehicle operational space as suggested by Fancher and Bareket (*27*). A vehicle trajectory can be visualized on this plot as a continuous line with a plausible direction of motion. The principle concerning the plausibility of the direction of motion is demonstrated with arrows in Figure 2*a*. The risk measures for a vehicle moving at 10 m/s, described by different safety indicators, are shown as a color map on this plot. In this study, the parameter values for w are $a_{max} = 3.3$ m/s^2, $t_s = 0.5$ s, $t_h = 1$ s, and $f(\mu) = 1$ and for PICUD are $a_{max} = 3.3$ m/s^2 and $t_h = 1$ s. This plot is used to visually examine the indicators for their validity and the risk variation along a trajectory. As shown in Figure 2*a*, iTTC is not defined for the lower quadrant, which describes a faster leader. PICUD and w have a smoother transition from "safe green" to "unsafe blue" than iTTC and SF. Moreover, the iTTC risk indication abruptly disappears in a transition from the upper to the lower quadrant of the plot.

SIMULATION EXPERIMENTS

The study is extended from theoretical findings to a simulation-based comparison of risk values associated with two-dimensional trajectories. In particular, peaks of the risk measures are examined, the ability to represent the risk related to vehicle maneuvers is analyzed, and the continuity of the risk measure over typical trajectories is inspected.

Two typical safety critical scenarios on highways are defined (*28*): emergency braking (Experiment 1) and cutting in (Experiment 2). The two experiments were done as a numerical simulation

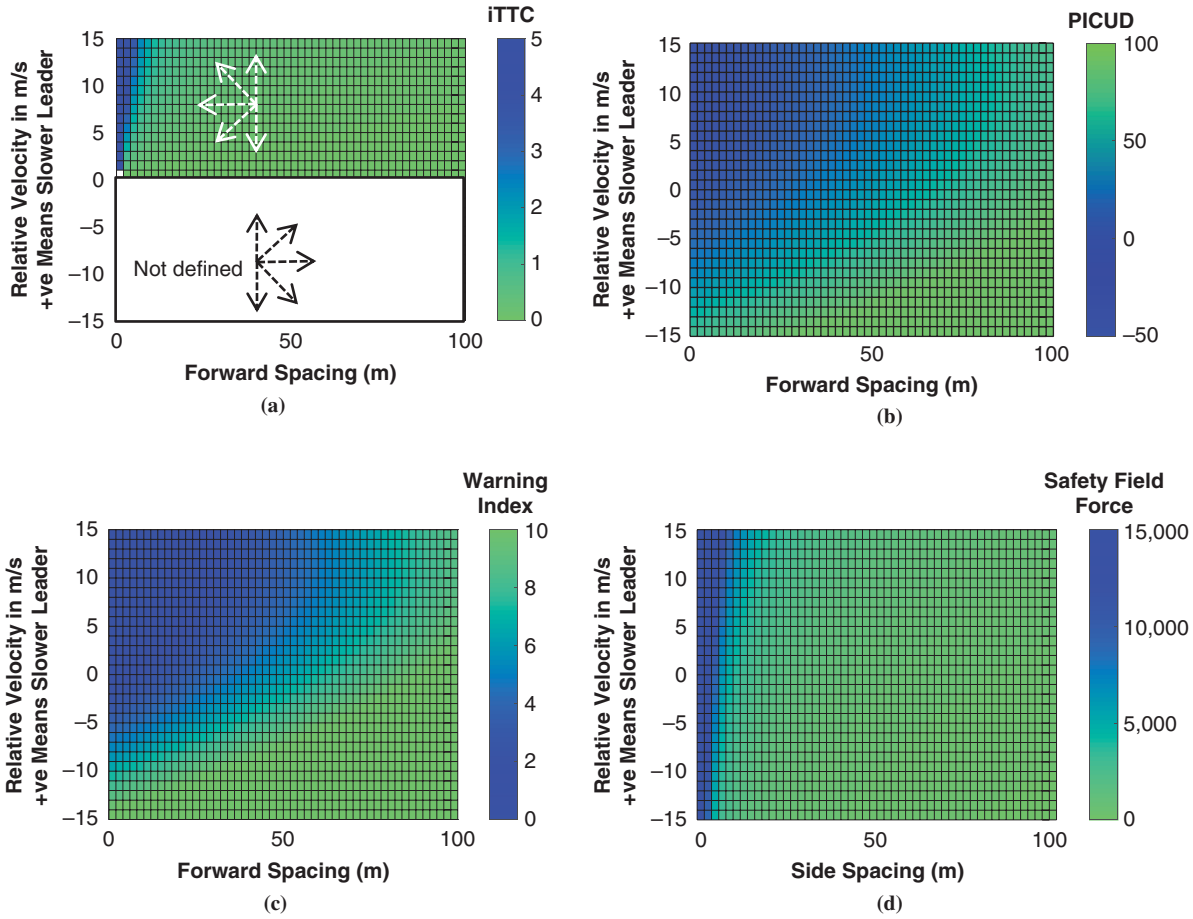

FIGURE 2 Visualization of risk measures over operational space using different safety indicators (blue indicates higher risk).

(a simulation time of 20 s and a time step of 0.2 s) of a vehicle pair: a leader with a predesigned trajectory to facilitate the scenario simulation and a follower. Longitudinal follower trajectories were simulated with the intelligent driver model with default parameters as in the original paper (*29*).

Another conservative simulation assumption used is that a vehicle would be identified as the leader only if it is ahead in the same lane. This assumption implies that a vehicle cutting in will be detected only after it crosses the lane boundary. The safety indicators considered are iTTC (threshold 0.5 s^{-1}) (*23*), PET (threshold 0.45 s), PICUD (threshold 0 m), and SF. These thresholds describe the safe ranges (*12, 23, 26*).

Experiment 1

In Experiment 1, a leader applying sudden braking (predefined) and three possible evasive maneuvers of the follower vehicle are simulated. Here, the leader vehicle traveling at 5 m/s and a spacing of 10.5 m ahead of the follower suddenly brakes (–2.5 m/s^2) at 5 s and reaches a complete halt at 7 s.

Figure 3*a* shows the risk profiles calculated with various safety indicators when the follower brakes to avoid a collision as dictated by the car-following intelligent drive model. It can be seen that iTTC is defined only in the time interval when the leader is slower than the follower. All three indicators depict an increasing risk measure as the leader brakes. PICUD and iTTC show the highest risk when the leader reaches a complete halt and thereafter the risk decreases, whereas SF indicates an increase in risk starting with the braking of the leader and reaches the maximum when the subject vehicle stops.

Trajectory planning systems often compare the risk levels of alternate trajectories to select the safer path (*5*). To verify if the selected indicators are capable of trajectory comparison, two evasive lane-change Trajectories A and B are simulated as possible alternative responses to the braking leader on a two-lane highway (one way). Figure 3*b* shows the risk profiles calculated with various safety indicators when the follower adopts Trajectory A. The follower Trajectory A begins with deceleration at 5.2 s in response to the lead vehicle's braking, followed by a left-lane change beginning at 5.4 s and ending at 9.6 s when the vehicle reaches the left lane center. Figure 3*c* shows the risk profiles calculated by using various safety indicators when the follower adopts Trajectory B (late lane change). The follower Trajectory B begins with deceleration at 5.2 s in response to the lead vehicle's braking, followed by a left-lane change beginning at 6.4 s and ending at the center of the left lane at 10.6 s. The lane change in two trajectories follows an S-shaped path defined by a fifth-degree polynomial parameterized by a lane change duration of 4.3 s, which is the typical value indicated by Samiee et al. (*30*), and a lateral displacement of 3.75 m, which is the typical lane width of a highway. The follower begins to acceler-

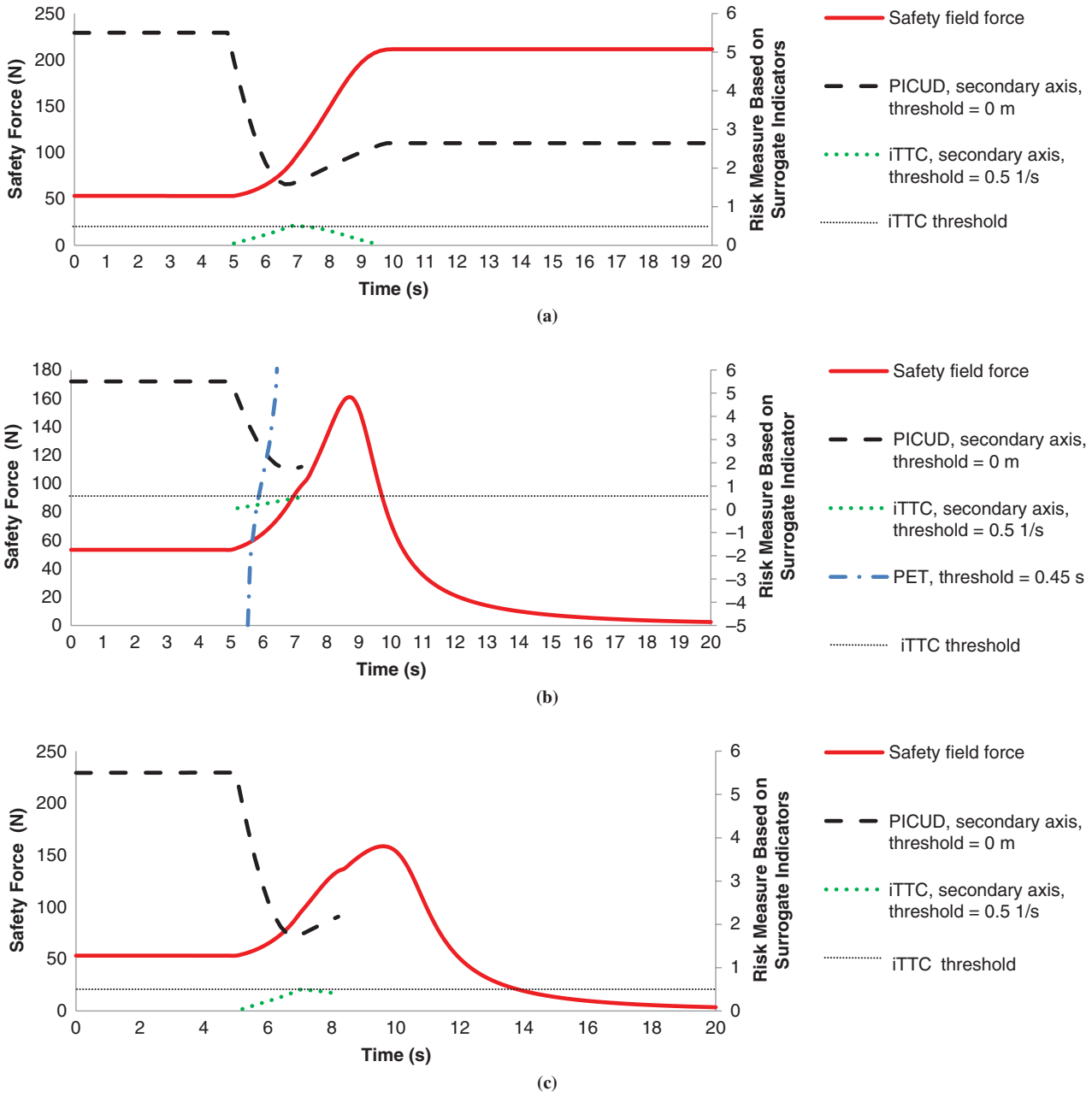

FIGURE 3 Results of Experiment 1: leader brakes and follower (*a*) brakes to avoid collision, (*b*) changes lanes via Trajectory A (timely lane change), and (*c*) changes lanes via Trajectory B (late lane change).

ate once the lane boundary is crossed and finally passes the leader on the adjacent lane at 9 s (Trajectory A) and 10.2 s (Trajectory B).

In both cases, PICUD and iTTC show an increasing risk while approaching; however, they were discontinued after the lane change. PET shows a decreasing risk starting from the beginning of the lane change via Trajectory A. SF shows continuous risk variation throughout the evasive maneuver and indicates the highest risk corresponding to a passing maneuver (Figure 3, *b* and *c*). The SF indicates a lower-risk peak for evasive lane change Trajectory A compared with evasive braking (Figure 3*a*). The total risk measure using SF (area under the plot) associated with Trajectory B (late lane change) is higher compared with Trajectory A (timely lane change). The other indicators cannot be used for comparison because they are discontinuous over the simulated trajectory.

Experiment 2

In Experiment 2, a three-lane highway (one way) was simulated with two vehicles (in right and middle lanes) moving with a forward spacing of 10.5 m. The vehicle traveling ahead in the right lane starts to cut in toward the middle lane at 2 s and reaches its center at 6.2 s. The two possible evasive maneuvers of the vehicle initially traveling behind on the middle lane are simulated. The risk profiles

(using selected indicators) when the follower brakes are shown in Figure 4*a*. PICUD and iTTC indicate the highest risk when the cut-in is detected and decreasing risk thereafter. PET indicates the highest risk earlier at the beginning of the cut-in and decreasing risk thereafter. SF indicates risk from the beginning of the cut-in; however, the highest risk is indicated at a later point when the cut-in vehicle reaches the center of the middle lane and thereafter it decreases.

Risk profiles (in terms of selected indicators) when the follower performs an evasive left-lane change are shown in Figure 4*b*. The follower begins to change lanes at 6.4 s and reaches the left-lane center at 10.6 s. PICUD and iTTC indicate the highest risk as the leader cut-in is detected. However, they are not defined during the evasive lane change since there is no leader in the left lane. PET indicates increasing (yet below threshold) risk with leader cut-in. SF indicates the highest risk for the passing maneuver (at 13.6 s) and reduced risk thereafter.

Findings of Simulation Analysis

- The point in time corresponding to the highest risk for a maneuver differs with the risk measure. For example, PICUD and TTC indicate the highest risk corresponding to the point of the cut-in, whereas the SF indicates the point of passing to be the riskiest (Figure 4).
- SSMs are defined for a collision course and hence have limited ability to capture the precautionary risk measures; in contrast, SF is able to indicate risk in the absence of a collision course, for example, a passing maneuver (Figures 3 and 4).
- SSMs are defined for the prescribed set of vehicle configurations and therefore indicate a sudden drop or rise in the risk profile during a change in this vehicle configuration. For example, the risk measures of TTC and PICUD increase suddenly when a vehicle is detected ahead (see Figure 4*b* at 4.6 s). In addition, from a control perspective, this is a false negative risk indication; that is, the indicator wrongly suggests zero risk for a vehicle cutting in ahead before being identified as a leader. SF is free of this drawback because it is independent of vehicle configuration assumptions.
- Even though PET and SF describe the risk profile of lateral maneuvers, the risk measures have limitations. The PET fluctuates throughout the maneuver (Figure 4*b*) and does not discriminate near-miss events in which a vehicle passes at a low lateral distance. In contrast, in the present formulation of SF, the intervehicle spacing has a high weight and therefore it consistently indicates the highest risk for a lateral vehicle passing even if both vehicles follow their lane center.

DISCUSSION OF RESULTS

As suggested in previous studies, the usefulness and validity of a safety indicator depends not only on the extent to which expected accident numbers can be correctly estimated but also on whether safety problems can be detected, road safety countermeasures

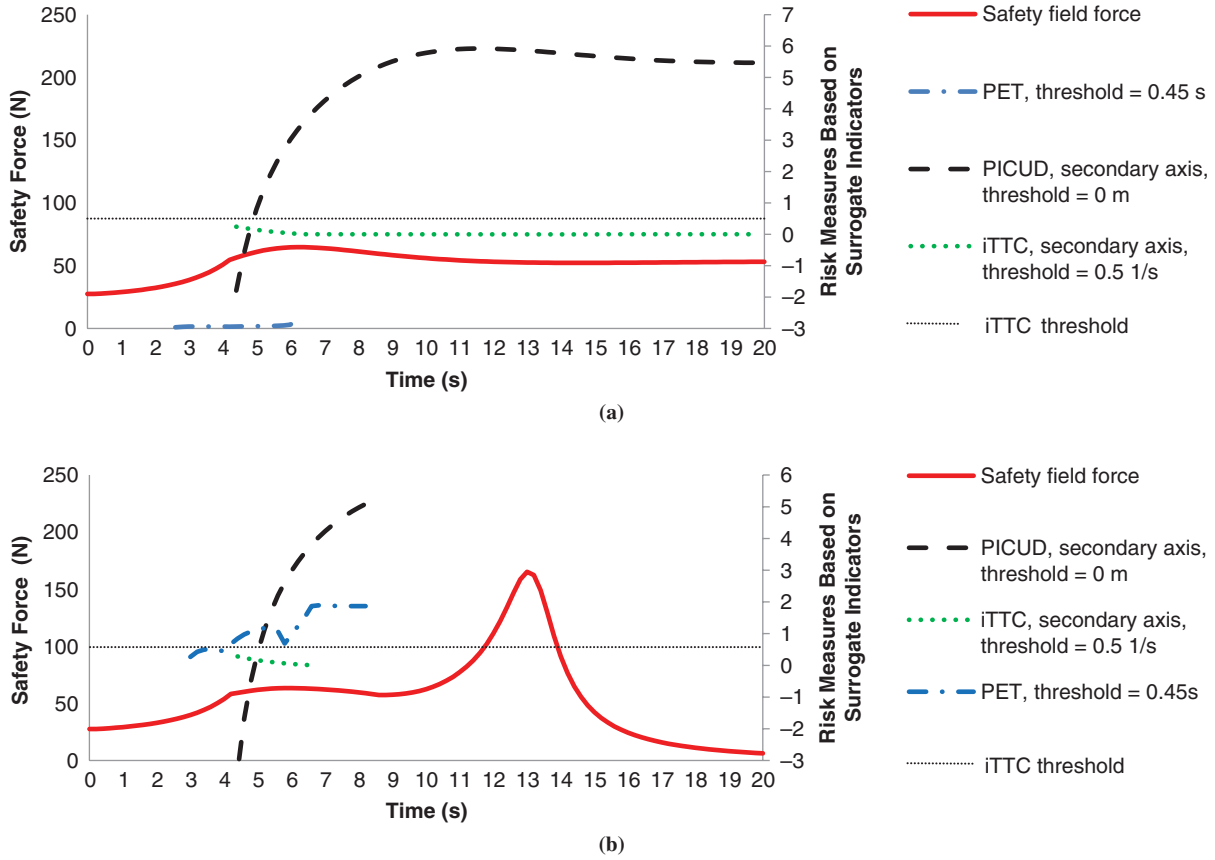

FIGURE 4 Results of Experiment 2: (*a*) leader cuts in and follower brakes to avoid collision and (*b*) follower changes lanes to avoid collision.

and treatments can be compared or evaluated, or both (*31*). In this study, the empirical validity was not explored. The indicators were reviewed on the basis of their ability to theoretically represent the expected risk tendencies and to evaluate safety problems along simulated trajectories in critical highway situations.

From the perspective of vehicle control systems accounting for safety utility, it is of interest to have smooth and objective risk measures (*32*). Simulation analysis showed that all the selected indicators are capable of delineating risk continuously in a one-dimensional interaction such as car following. However, SSMs like iTTC, PET, *w,* and PICUD often display fluctuating or discontinuous values, or both. For example, iTTC (and TTC) change abruptly when crossing the line of $\Delta v = 0$ (Figure 2). The measured relative speed may oscillate from positive to negative because of sensing errors, and this fluctuation will result in changing risk measures and in turn the control signals based on them. Moreover, as shown in the simulation analysis, discontinuous risk measures cannot be used in trajectory planners to compare alternate trajectories. Second, these indicators do not possess mathematical properties that are desirable in a multivehicle scenario. Third, benchmarking the safety level based on an indicator threshold value is difficult because of the limited number of parameters considered by these indicators (*16, 26*). The threshold may vary with road characteristics, interacting vehicle type, and driver reaction time. For example, a TTC that is considered safe on a high-friction road could be deemed unsafe on a low-friction or icy road. Moreover, most of the SSMs do not account for conflict severity. Hence, the decision-making modules of intelligent vehicles that use these indicators cannot identify the trajectory of lesser crash severity in an unavoidable collision situation. Finally, as shown in the simulation analysis, indicators defined for a prescribed set of vehicle interaction configurations often lead to false negative risk measures.

These findings also have implications for the use of safety indicators for traffic safety assessment. The one-dimensional safety indicators yield partial insights on safety because they are only valid for a predefined set of vehicle interactions and do not account for collision severity. Also, these indicators cannot be used to estimate collective risk because they do not possess the property of countable additivity. As reported in the simulation results, SSMs differ on the basis of the threshold definition and underlying kinematic assumptions. This feature makes it difficult to reach an objective consensus on the safety impact. Finally, the limitations of the lateral indicators like fluctuation (PET) and sensitivity to spacing (SF) question the objectivity of safety assessments for multilane highways. SF can potentially be used to model precautionary measures taken by human drivers because it can describe risk despite a collision course.

All the studied safety indicators are based on underlying deterministic assumptions on the future kinematic state of the interacting vehicles rather than acknowledgment of the uncertainty in vehicle movement. For example, in a scenario where a vehicle follows a leader at a spacing of 1 m, the scenario would be deemed safe by a TTC indicator that is based on the assumption of constant velocity. However, this scenario cannot be regarded as safe if the probability that the leader may brake is considered. Even though the SF approach does not depend on kinematic assumptions, it also does not explicitly account for uncertainties. Moreover, autonomous vehicles further contribute to the necessity of accounting for vehicle uncertainty in risk measures. Autonomous vehicles may attain more precise control as compared with manual driving and may thereby safely pass at short distances; however, the precision of an autonomous vehicle will be affected by its perception quality. Therefore, this lack of consideration of uncertainties related to the vehicle's state is a drawback of these indicators.

This study demonstrates the advantages of the SF framework in depicting the risk of two-dimensional vehicle interactions. Recently, Wang et al. demonstrated the use of an SF-based indicator for collision warning applicable in multivehicle scenarios (*33*). Moreover, if augmented with prediction paradigms, SF can be used for ex ante safety evaluation in path planners. However, the formulation has to be fine-tuned, refined, or both, for practical applications. Unlike the SSM, SF does not represent the collision causal mechanism, and therefore interpretation of the SF risk measure could become ambiguous.

CONCLUSION AND FUTURE WORK

In this study safety indicators were compared on the basis of their qualitative and quantitative aspects as a risk measure. The results showed that all the selected indicators are capable of delineating risk continuously in a one-dimensional interaction like car following. Moreover, the selected safety indicators in general match the expected risk tendencies. However, in agreement with previous research (*6, 10–13*), the current findings acknowledge the mathematical limitations of selected safety indicators like discontinuity over the operational space, omission of uncertainty in vehicle state assumptions, and the inability to account for crash severity. Also, all these indicators lack mathematical properties to account for multiple vehicles and the SF framework is a promising approach that allows risk estimation in two-dimensional vehicle interactions. This analysis could be further improved by verifying the findings with empirical accident data. Future research should also focus on defining a safety indicator that addresses the limitations of existing indicators found in this study.

ACKNOWLEDGMENT

This work was supported by STW Technology Foundation, in the Netherlands, under the project From Individual Automated Vehicles to Cooperative Traffic Management (IAVTRM).

REFERENCES

1. *Global Status Report on Road Safety, 2015.* World Health Organization, Geneva, 2015.
2. Archer, J. *Indicators for Traffic Safety Assessment and Prediction and Their Application in Micro-Simulation Modelling: A Study of Urban and Suburban Intersections.* PhD dissertation. Royal Institute of Technology, Stockholm, Sweden, 2005.
3. Azevedo, C. L., and H. Farah. Using Extreme Value Theory for the Prediction of Head-On Collisions During Passing Maneuvers. In *Proceedings of IEEE International Conference on Intelligent Transportation Systems,* IEEE, New York, 2015, pp. 268–273. https://doi.org/10.1109/ITSC.2015.53.
4. Wilmink, I. R., G. A. Klunder, and B. van Arem. Traffic Flow Effects of Integrated Full-Range Speed Assistance (IRSA). In *Proceedings of the IEEE Intelligent Vehicles Symposium,* IEEE, New York, 2007, pp. 1204–1210. https://doi.org/10.1109/IVS.2007.4290282.
5. Wang, M., S. P. Hoogendoorn, W. Daamen, B. van Arem, and R. Happee. Game Theoretic Approach for Predictive Lane-Changing and Car-Following Control. *Transportation Research Part C: Emerging Technologies,* Vol. 58, 2015, pp. 73–92. https://doi.org/10.1016/j.trc.2015.07.009.

6. Kuang, Y., X. Qu, and S. Wang. A Tree-Structured Crash Surrogate Measure for Freeways. *Accident Analysis and Prevention,* Vol. 77, 2015, pp. 137–148. https://doi.org/10.1016/j.aap.2015.02.007.
7. Kiefer, R.J., C.A. Flannagan, and C.J. Jerome. Time-to-Collision Judgments Under Realistic Driving Conditions. *Journal of the Human Factors and Ergonomics Society,* Vol. 48, No. 2, 2006, pp. 334–345. https://doi.org/10.1518/001872006777724499.
8. Wang, J., J. Wu, and Y. Li. The Driving Safety Field Based on Driver–Vehicle–Road Interactions. *IEEE Transactions on Intelligent Transportation Systems,* Vol. 16, No. 4, 2015, pp. 2203–2214. https://doi.org/10.1109/TITS.2015.2401837.
9. Svensson, Å. *A Method for Analysing the Traffic Process in a Safety Perspective.* PhD dissertation. Lund Institute of Technology, Sweden, 1998.
10. Zheng, L., K. Ismail, and X. Meng. Traffic Conflict Techniques for Road Safety Analysis: Open Questions and Some Insights. *Canadian Journal of Civil Engineering,* Vol. 41, No. 7, 2014, pp. 633–641. https://doi.org/10.1139/cjce-2013-0558.
11. Young, W., A. Sobhani, M.G. Lenné, and M. Sarvi. Simulation of Safety: A Review of the State of the Art in Road Safety Simulation Modelling. *Accident Analysis and Prevention,* Vol. 66, 2014, pp. 89–103. https://doi.org/10.1016/j.aap.2014.01.008.
12. van Beinum, A., H. Farah, F. Wegman, and S. Hoogendoorn. Critical Assessment of Methodologies for Operations and Safety Evaluations of Freeway Turbulence. *Transportation Research Record: Journal of the Transportation Research Board,* No. 2556, 2016, pp. 39–48. https://doi.org/10.3141/2556-05.
13. Gettman, D., and L. Head. Surrogate Safety Measures from Traffic Simulation Models. *Transportation Research Record: Journal of the Transportation Research Board,* No. 1840, 2003, pp. 104–115. http://dx.doi.org/10.3141/1840-12.
14. Minderhoud, M.M., and P.H.L. Bovy. Extended Time-to-Collision Measures for Road Traffic Safety Assessment. *Accident Analysis and Prevention,* Vol. 33, No. 1, 2001, pp. 89–97. https://doi.org/10.1016/S0001-4575(00)00019-1.
15. Jula, H., E.B. Kosmatopoulos, and P.A. Ioannou. Collision Avoidance Analysis for Lane Changing and Merging. *IEEE Transactions on Vehicular Technology,* Vol. 49, No. 6, 2000, pp. 2295–2308. https://doi.org/10.1109/25.901899.
16. Damerow, F., and J. Eggert. Predictive Risk Maps. In *Proceedings of the IEEE Conference on Intelligent Transportation Systems,* IEEE, New York, 2014, pp. 703–710. https://doi.org/10.1109/ITSC.2014.6957772.
17. Evans, L.C., and R.F. Gariepy. *Measure Theory and Fine Properties of Functions.* Studies in Advanced Mathematics. CRC Press, Boca Raton, Fla., 1991.
18. Aarts, L., and I. Van Schagen. Driving Speed and the Risk of Road Crashes: A Review. *Accident Analysis and Prevention,* Vol. 38, No. 2, 2006, pp. 215–224. https://doi.org/10.1016/j.aap.2005.07.004.
19. Evans, L. Driver Injury and Fatality Risk in Two-Car Crashes Versus Mass Ratio Inferred Using Newtonian Mechanics. *Accident Analysis and Prevention,* Vol. 26, No. 5, 1994, pp. 609–616. https://doi.org/10.1016/0001-4575(94)90022-1.
20. Laureshyn, A., T. De Ceunynck, C. Karlsson, Å. Svensson, and S. Daniels. In Search of the Severity Dimension of Traffic Events: Extended Delta-V as a Traffic Conflict Indicator. *Accident Analysis and Prevention,* Vol. 98, 2017, pp. 46–56. https://doi.org/10.1016/j.aap.2016.09.026.
21. Othman, S., and R. Thomson. Influence of Road Characteristics on Traffic Safety. In *Proceedings: 21st International Technical Conference on the Enhanced Safety of Vehicles (ESV),* NHTSA, U.S. Department of Transportation, 2009, pp. 1–10.
22. Klauer, S.G., T.A. Dingus, V.L. Neale, J.D. Sudweeks, and D.J. Ramsey. *The Impact of Driver Inattention on Near Crash/Crash Risk: An Analysis Using the 100-Car Naturalistic Driving Study Data.* Report DOT HS 810 594. NHTSA, U.S. Department of Transportation, 2006.
23. Moon, S., I. Moon, and K. Yi. Design, Tuning, and Evaluation of a Full-Range Adaptive Cruise Control System with Collision Avoidance. *Control Engineering Practice,* Vol. 17, No. 4, 2009, pp. 442–455. https://doi.org/10.1016/j.conengprac.2008.09.006.
24. Fancher, P., Z. Bareket, and R. Ervin. Human-Centered Design of an Acc-With-Braking and Forward-Crash-Warning System. *Vehicle System Dynamics,* Vol. 36, No. 2-3, 2001, pp. 203–223. https://doi.org/10.1076/vesd.36.2.203.3557.
25. Zheng, L., K. Ismail, and X. Meng. Freeway Safety Estimation Using Extreme Value Theory Approaches: A Comparative Study. *Accident Analysis and Prevention,* Vol. 62, 2014, pp. 32–41. https://doi.org/10.1016/j.aap.2013.09.006.
26. Ni, D. A Unified Perspective on Traffic Flow Theory, Part 1: The Field Theory. *Applied Mathematical Sciences,* Vol. 7, 2013, pp. 1929–1946.
27. Fancher, P.S., and Z. Bareket. Evaluating Headway Control Using Range Versus Range-Rate Relationships. *Vehicle System Dynamics,* Vol. 23, No. 1, 1994, pp. 575–596. https://doi.org/10.1080/00423119408969076.
28. Hyden, C. *The Development of a Method for Traffic Safety Evaluation: The Swedish Traffic Conflicts Technique.* Bulletin 70. Lund Institute of Technology, Lund, Sweden, 1987.
29. Treiber, M., A. Hennecke, and D. Helbing. Congested Traffic States in Empirical Observations and Microscopic Simulations. *Physical Review,* Vol. 62, No. 2, 2000, pp. 1805–1824.
30. Samiee, S., S. Azadi, R. Kazemi, and A. Eichberger. Towards a Decision-Making Algorithm for Automatic Lane Change Manoeuvre Considering Traffic Dynamics. *Promet – Traffic&Transportation,* Vol. 28, No. 2, 2016, pp. 91–103.
31. Laurenshyn, A., and P. Olszewski. *Review of Current Study Methods for VRU Safety.* Appendix 6: *Scoping Review: Surrogate Measures of Safety in Site-Based Road Traffic Observations.* Deliverable 2.1–Part 4. Horizon 2020, European Commission, Brussels, Belgium, 2016.
32. Mullakkal-Babu, F.A., M. Wang, B. Van Arem, and R. Happee. Design and Analysis of Full Range Adaptive Cruise Control with Integrated Collision Avoidance Strategy. In *Proceedings of IEEE International Conference on Intelligent Transportation Systems,* IEEE, New York, 2016, pp. 308–315.
33. Wang, J., J. Wu, X. Zheng, D. Ni, and K. Li. Driving Safety Field Theory Modeling and Its Application in Pre-Collision Warning System. *Transportation Research Part C: Emerging Technologies,* Vol. 72, 2016, pp. 306–324. https://doi.org/10.1016/j.trc.2016.10.003.

The Standing Committee on Safety Data, Analysis, and Evaluation peer-reviewed this paper.